

# Non-Abelian topological insulators from an array of quantum wires

Eran Sagi and Yuval Oreg

*Department of Condensed Matter Physics, Weizmann Institute of Science, Rehovot, Israel 76100*

(Dated: December 6, 2024)

We suggest a construction of a large class of topological states using an array of quantum wires. First, we show how to construct a Chern insulator using an array of alternating wires that contain electrons and holes, correlated with an alternating magnetic field. This is supported by semi-classical arguments and a full quantum mechanical treatment of an analogous tight-binding model. We then show how electron-electron interactions can stabilize fractional Chern insulators (Abelian and non-Abelian). In particular, we construct a relatively stable non-Abelian  $\mathbb{Z}_3$  parafermion state. Our construction is generalized to wires with alternating spin-orbit couplings, which give rise to integer and fractional (Abelian and non-Abelian) topological insulators. The states we construct are effectively two-dimensional, and are therefore less sensitive to disorder than one-dimensional systems. The possibility of experimental realization of our construction is addressed.

PACS numbers: 73.21.Hb, 71.10.Pm, 73.43.-f, 05.30.Pr

*Introduction:* The integer quantum Hall effect (IQHE) [1] was discovered in two-dimensional (2D) systems subjected to a strong perpendicular magnetic field. The quantized conductance is a consequence of the emergence of a topological number [2], known as the Chern number. Haldane [3] showed that a Graphene-like material which breaks time-reversal symmetry due to an alternating (zero average) magnetic field may have a non-zero Chern number as well. These types of materials, which have a non-zero Hall conductance with a zero total magnetic flux, are referred to as Chern insulators (CI).

The existence of edge modes [4] in the QHE can be understood in various ways. In particular, one can understand the presence of edge modes by studying the classical curved trajectories of electrons in a magnetic field. In fact, it is possible to construct a semi-classical theory for a specific set of Chern insulators as well. Consider a system consisting of electrons and holes, whose masses differ in sign. In the presence of a magnetic field, their classical trajectories are curved in opposite directions. If however, the electrons and the holes experience opposite magnetic fields, the trajectories will be curved in the same direction. One can imagine constructing a Chern-insulator by separating the planes into regions which contain only holes and only electrons. If the magnetic field is opposite in the two regions, the classical trajectories will be similar to those of electrons in a uniform magnetic field. This suggests that, upon quantization, this system should have a non-zero Chern number [5].

Motivated by this semi-classical picture, we will study in this work an effectively 2D system which consists of alternating wires that contain electrons and holes. Approaching the 2D problem from the quasi-one-dimensional (Q1D) limit enables a full quantum-mechanical analysis, and an analytic treatment of interaction effects using the bosonization technique. Ref. [6, 7] argues that it is possible to understand the IQHE by considering a set of weakly coupled parallel wires. First,

we will show that one can use an array of wires to construct a CI as well (see Fig. 1a). We then introduce a tight-binding version of this model and obtain a phase diagram, showing the Chern number as a function of the model parameters.

Kane et al. [8] generalized the wires approach to the Abelian fractional quantum Hall effect (FQHE) using the bosonization technique. We will generalize our construction to a fractional CI (FCI) as well.

To do so, we introduce composite particles. This transformation maps the electrons and holes at  $1/3$  filling to composite particles at filling 1. The possibility of a FCI has recently been discussed quite extensively in the literature [9]. Numerical investigations [10–15] of lattice models with nearly flat bands presented strong evidence for FCI states. More general approaches, connecting the properties of the known FQHE states and analogous FCI states, were found [16, 17]. Here we present an alternative analytic approach to the subject, which may be applicable in experiments.

Teo & Kane [18] expand the approach of [8] to non-Abelian states. We will see that our results can be generalized to the non-Abelian case as well, and we will provide a detailed construction of a state similar to the  $\mathbb{Z}_3$  Read-Rezay state. This state supports Fibonacci anyons, which may be used for universal quantum computation [19, 20]. We expect this construction to be rather stable, as it is built from effective  $\nu = 1/3$  states.

Using an analogy between a magnetic field and a spin-orbit coupling (in the  $\hat{z}$  direction only), we will construct a topological insulator from an array of wires using an alternating spin-orbit coupling.

We note that the Q1D approach was recently used by various papers [26–28] to discuss a variety of topological states.

*Wires construction of a CI:* Motivated by the above semi-classical picture, we have designed the wires construction, shown in Fig. 1a. In each unit cell there are

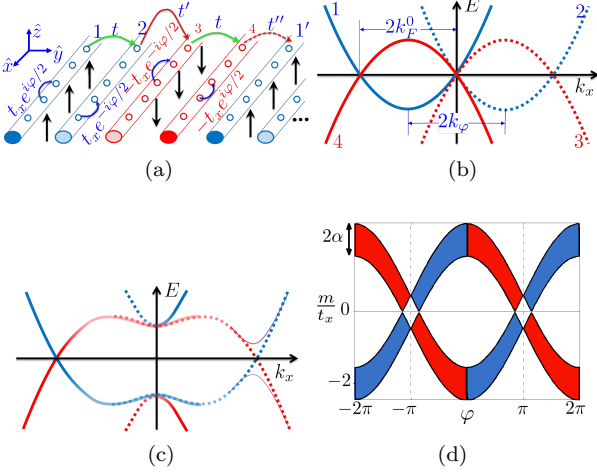


FIG. 1. (Color Online) (a) Physical scheme of the Q1D model we study. Blue wires contain electrons, and red wires contain holes. The black arrows represent the magnetic field through the system. The circles represent the sites of the corresponding tight binding model, and the tunneling amplitudes of the tight binding model are represented by colored arrows. (b) The energy spectrum of the wires (as a function of  $k_x$ ) near zero energy without tunneling between the wires ( $t, t', t'' = 0$ ). The mass term is chosen such that the four parabolas cross each other at zero energy. The spectra in blue, dashed blue, dashed red, and red correspond to wires 1, 2, 3, and 4 in a unit cell, respectively.  $k_F^0$  is the Fermi  $k$ -vector in the absence of a magnetic field, and  $k_\varphi a = \varphi/2$  is the shift of the spectra due to the magnetic field. (c) Thick lines show the energy spectrum when  $t$  is switched on. A gap opens near  $k_x = 0$ . The thin full lines show the spectrum when  $t'$  is switched on as well. This gives an additional gap at  $k_x > 0$ . Free chiral modes are left on wires 1 and 4. Finally, if one switches on  $t''$ , there are free chiral modes at the edge of the system, which suggests that there is a non-zero Chern number. (d) The phase diagram showing the Chern number as a function of  $m$  and  $\varphi$ . Red regions have  $C = 1$ , blue regions have  $C = -1$ , and white regions are topologically trivial regions with  $C = 0$ . The figure was generated with the parameters  $t/t_x = 0.5, t'/t_x = t''/t_x = 0.2$ .

four different wires. We tune the wires' chemical potentials such that wires 1 and 2 of each unit cell are near the bottom of the band, and wires 3 and 4 are near the top. Effectively, we have alternating pairs of wires that contain electrons and holes. A positive (negative) magnetic field is introduced between the pairs of electron (hole) wires. This is a Q1D version of the semi-classical picture we described above.

For illustration and simplicity it is convenient to choose a gauge in which the vector potential  $\mathbf{A}$  points at the  $x$  direction. We can tune the wires' bands in such a way that all their crossing points match in energy. In this case, the energy spectra are similar to those depicted in Fig. 1b.

If in addition, neighboring wires of the same type are weakly tunnel coupled (with an amplitude  $t$ ), a gap opens

between parabolas 1 and 2, and parabolas 3 and 4. The spectrum in this case is depicted by the thick lines of Fig. 1c.

Introducing now a coupling between the electrons and holes *inside* a unit cell ( $t'$ ), a gap will open at  $k_x > 0$ , and we arrive at the spectrum depicted by the thin lines of Fig. 1c. If we now switch on small tunneling between different unit cells ( $t''$ ), the coupling between the edges decays exponentially with the sample width, and in the thermodynamic limit we expect to find gapless edge states. The observation of gapless edge states indicates that there is a non-zero Chern number.

**Tight binding Model:** To show this explicitly, we have constructed a 2D tight-binding model, which is the lattice version of the above continuous model (for more details see the supplemental material [29]). We introduce the nearest neighbor tunneling amplitudes:  $t, t', t'', \pm t_x e^{\pm i k_\varphi a}$ , described in Fig. 1a. The phase  $e^{\pm i k_\varphi a}$ , with  $k_\varphi a = \frac{e B a^2}{2 \hbar c}$ , is the Peierls phase associated with the alternating external magnetic field. It is related to the flux in a basic unit cell:  $k_\varphi a = \frac{\varphi}{2}$ , where  $\varphi = 2\pi \frac{\Phi}{\Phi_0}$ . In addition, we introduce a mass term (not related to the physical mass of the particle), which adds a constant energy  $m$  ( $-m$ ) for electrons (holes). The sign of  $t_x$  is equal to the sign of the mass term. Similar to Haldane's original model [3],  $m$  and  $\varphi$  tune the system into and out of the topological phases.

For simplicity, we restrict ourselves to the case  $t'' = t'$ . Using the particle-hole and inversion symmetries of the resulting Hamiltonian, we can find that the upper and lower bands cross each other when  $\frac{m}{t_x} = \pm 2 \cos \frac{\varphi}{2} \pm \alpha$ , with  $\alpha = \sqrt{t^2 - t'^2}/t_x$  [29] (in addition to the trivial crossings at  $\varphi = 0, 2\pi$ ). These crossing points signal a topological phase transition between a trivial insulator and a Chern insulator. The full phase diagram, showing the Chern number as a function of  $\varphi$  and  $m$ , is depicted in Fig. 1d. We note that if we break the built-in particle-hole symmetry of the model by adding a small chemical potential  $\mu$ , metallic phases appear between the trivial and the Chern insulating phases. The boundaries of these metallic regions are  $\frac{m}{t_x} = \pm 2 \cos \frac{\varphi}{2} \pm \alpha_\pm$ , where  $\alpha_\pm = \sqrt{(t \pm \mu)^2 - t'^2}/t_x$ .

**FCI:** The wires construction invites us to add interactions and use bosonization techniques, similar to those used in [8, 18]. This allows us to generalize the above results to FCI states. In the presence of interactions, multi-electron processes may open a gap even if the Fermi point of the left movers is not equal to the Fermi points of the right movers [8, 18, 21, 22].

To understand the required conditions for a gap opening due to multi-electron scattering processes, it is useful to present the spectra of Fig. 1b in an alternative way. Instead of plotting the entire spectrum of the wires together, we plot only the Fermi points as a function of the wire index. Soon, we will linearize the spectra

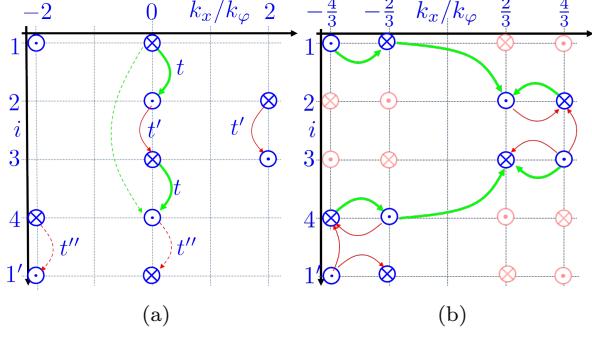


FIG. 2. (Color Online) (a) A diagrammatic representation of the energy band structure in the case  $\nu \equiv k_F^0/k_\varphi = 1$  (See Fig. 1b for definitions of  $k_\varphi$  and  $k_F^0$ ). The  $y$  axis shows the wire index inside the unit cell, and the  $x$  axis shows  $k_x$  in units of  $k_\varphi$ . The symbol  $\odot$  ( $\otimes$ ) represents  $k_i^L$  ( $k_i^R$ ). Colored arrows represent tunneling amplitudes between the wires. (b) The same diagram for a topological insulator with  $\nu = \frac{1}{3}$ . Colored arrows now represent the multi-electron processes responsible for the creation of Laughlin-like states. These complex processes in terms of the electrons ( $\psi \sim e^{i\phi}$ ) for  $\nu = 1/3$  are mapped to simple tunneling processes in terms of the fermions  $\tilde{\psi} \sim e^{i\eta}$ . Thus,  $\nu = 1/3$  for  $\psi$  is equivalent to  $\nu = 1$  for  $\tilde{\psi}$ . In the presence of spin orbit coupling, spin up (blue) and spin down (light red) will experience opposite alternating effective magnetic fields.

around these points. A cross ( $\otimes$ ) denotes the Fermi point of a right mover, and a dot ( $\odot$ ) denotes the Fermi point of a left mover. Before analyzing the fractional case, it is useful to revisit the simple  $\nu = 1$  case. We will see that the main results of the tight binding model arise naturally in the bosonization framework. Fig. 2a shows the diagram that corresponds this case (Fig. 1b). Linearizing the spectrum around the Fermi-points of each wire, and using the standard bosonization procedure, we define the two chiral bosonic fields,  $\phi_i^R$  and  $\phi_i^L$ , for each wire. In terms of these, the fermionic operators are  $\psi_i^R \propto e^{i(k_i^R x + \phi_i^R)}$ ,  $\psi_i^L \propto e^{i(k_i^L x + \phi_i^L)}$ .

Without interactions, a momentum conserving single-electron tunneling between the wires (denoted in Fig. 2a by an arrow) is possible only when the left and right movers of adjacent wires are at the same point in  $k$ -space. The single-electron tunneling operators between adjacent wires (denoted in Fig. 2a by green, red, and dashed red arrows) are

$$\begin{aligned} t\psi_{1(3)}^{R\dagger}\psi_{2(4)}^L + h.c. &\propto t \cos(\phi_{1(3)}^R - \phi_{2(4)}^L), \\ t'\psi_2^{R(L)\dagger}\psi_3^{L(R)} + h.c. &\propto t' \cos(\phi_2^{R(L)} - \phi_3^{L(R)}), \\ t''\psi_4^{R(L)\dagger}\psi_{1'}^{L(R)} + h.c. &\propto t'' \cos(\phi_4^{R(L)} - \phi_{1'}^{L(R)}). \end{aligned} \quad (1)$$

We switch on the operators in the following way: first, we switch on a small  $t \ll t_x$ . Since this is a relevant operator, it gaps out the spectrum near  $k_x = 0$ . Then, we switch

on smaller electron-hole couplings  $t', t'' < t$ . The terms  $\psi_2^{R\dagger}\psi_3^L$  and  $\psi_4^{R\dagger}\psi_{1'}^L$  gap out the rest of the spectrum, leaving a gapless edge mode. As we discussed before, this indicates that there is a non-zero Chern number. Note that the terms  $\psi_2^{L\dagger}\psi_3^R$  and  $\psi_4^{L\dagger}\psi_{1'}^R$  contain fields which are conjugate to those already pinned by  $t$ . Strong quantum fluctuations are therefore expected to suppress these terms.

We now turn to generalize this to Laughlin-like FCI states, with a filling factor  $\nu = k_F^0/k_\varphi = 1/(2n+1)$ , where  $n$  is a non-negative integer. For example, the  $k$ -vector pattern of the wires with  $\nu = 1/3$  is shown in blue in Fig. 2b. In this case, multi-electron processes are expected to gap out the system (except for the edges). To see this, it is enlightening to define new chiral fermion operators

$$\tilde{\psi}_i^{R(L)} = (\psi_i^{R(L)})^{(n+1)} (\psi_i^{\dagger L(R)})^n \propto e^{i(q_i^{R(L)}x + \eta_i^{R(L)})}, \quad (2)$$

with

$$\eta_i^{R(L)} = (n+1)\phi_i^{R(L)} - n\phi_i^{L(R)}, \quad (3)$$

and  $q_i^{R(L)} = (n+1)k_i^{R(L)} - nk_i^{L(R)}$ . A direct calculation of the commutation relations of the  $\eta$ -fields show that they have an additional factor of  $2n\pi$  compared the  $\phi$ -fields. This gives an extra (trivial) phase factor  $e^{i2\pi n}$  in the anti-commutation relation of the  $\tilde{\psi}$ 's compared to the  $\psi$ 's, insuring that the  $\tilde{\psi}$ 's are fermionic operators. In addition, it can easily be checked that the resulting structure of the  $q$ 's is identical to that of the  $k$ 's in the case of  $\nu = 1$  (Fig. 2a), so that  $\tilde{\psi}$  can be regarded as a fermionic field with  $\nu = 1$ . This procedure can therefore be interpreted as an attachment of  $2n$  quantum fluxes to each electron (similar to Jain's construction of composite fermions [30]).

Repeating the analysis of the  $\nu = 1$  case, we can now write single  $\tilde{\psi}$  tunneling operators, identical to those found in Eq. (1) (replacing  $\psi \rightarrow \tilde{\psi}$ ,  $\phi \rightarrow \eta$ , with new tunneling amplitudes  $\tilde{t}$ ,  $\tilde{t}'$ , and  $\tilde{t}''$ ). In terms of the original electrons, these operators describe the multi-electron processes shown in Fig. 2b. Note that when the interactions are strong enough, these operators become relevant. From here, the process is identical to the integer case. The gap due to the  $\tilde{\psi}$  tunneling operators insures that competing processes (for example, single electron tunneling between wires 2 and 3, or 4 and 1') are suppressed, as they contain fields that are conjugate to the fields pinned by  $\tilde{t}$  (which is dominant by our construction).

The fact that the composite  $\eta$ -fields (and not the original  $\phi$  fields) are pinned, leads to the various properties of these Laughlin-like states, like the fractional charge and statistics of the excitations, in analogy to the known FQHE states [8, 18].

*Non-Abelian FCI:* As the discussion above shows, the wires construction allowed us to create Abelian fractional

Chern insulators. Ref. [18] constructed non-Abelian QHE states by enlarging the unit cell, and taking a non-uniform magnetic field inside each unit cell. By our construction, any non-Abelian state constructed by [18] can be generalized to the CI case. To do so, one can take two unit cells from the construction in Ref. [18], reverse the magnetic field of the second unit cell, and use holes instead of electrons. However, the lack of a total magnetic flux in our system enables a simpler construction of non-Abelian states, which don't have a direct analog in the QHE. We now show that a slight modification of the procedure that enabled the construction of Laughlin-like states may lead to non-Abelian states. We will focus here on a state similar to the  $\mathbb{Z}_3$  Read-Rezay state. Generalization to other non-Abelian states is possible.

To obtain a  $\mathbb{Z}_3$  parafermion state, we take  $\nu = 1/3$ , and construct the  $\tilde{\psi}$  operators. We switch on first the  $\tilde{t}'$  term, which leaves free  $\tilde{\psi}$ -fields on wires 1 and 4. If we now switch on smaller  $\tilde{t}$  terms, we generate (in second order perturbation theory) an effective coupling of order  $\tilde{t}^2/\tilde{t}'$  between  $\tilde{\psi}_1^R$  and  $\tilde{\psi}_4^L$  (See dashed green line in Fig. 2a). If we approach the limit  $\tilde{t}' \sim \tilde{t}$ , we find that  $\tilde{t}^2/\tilde{t}' \sim \tilde{t}$ , so that the four operators  $\tilde{\psi}_1^{\dagger R} \tilde{\psi}_4^L$ ,  $\tilde{\psi}_1^{\dagger R} \tilde{\psi}_2^L$ ,  $\tilde{\psi}_3^{\dagger R} \tilde{\psi}_2^L$  and  $\tilde{\psi}_3^{\dagger R} \tilde{\psi}_4^L$  have similar amplitudes. Let us assume that we tune  $\tilde{t}, \tilde{t}'$ , and the coupling between  $\tilde{\psi}_1^R$  and  $\tilde{\psi}_4^L$ , to have exactly the same value, denoted by  $v$  (at the end, when the topological nature of our construction will be revealed, this strict requirement can be relaxed, as long as the bulk gap doesn't close). It can be shown (see supplemental material [29]) that under these assumptions our problem is mapped to the  $\beta^2 = 6\pi$  self-dual Sine-Gordon model, which was studied in Ref. [25, 31]. Specifically, it was shown that this model is mapped to a critical  $\mathbb{Z}_3$  parafermionic field.

We have established that any unit cell has two counter propagating  $\mathbb{Z}_3$  parafermionic fields (around  $k = 0$ ), and two counter propagating charge modes at  $k_x = -2k_\varphi$ . As earlier, we can gap out the spectrum by switching on the  $t''$  term between the unit cells, leaving eventually a Laughlin-like charge mode and a  $\mathbb{Z}_3$  parafermion mode at the edge of the sample. We note that while the non-Abelian part is the same as the non-Abelian part of the  $\mathbb{Z}_3$  Read-Rezay state, the charge mode is different.

*Topological insulators from the wires approach:* The entire analysis presented here can also be carried out for spinful electrons if one introduces spin-orbit interactions (in the  $\hat{z}$  direction only). This can be done if an alternating electric field is introduced instead of an alternating magnetic field. For example, the electric field can be tuned in such a way that the spin-orbit coupling is positive at wires 1 and 4, and negative at wires 2 and 3. Fig. 2b shows the appropriate Fermi-momenta corresponding to  $\nu = \frac{1}{3}$  (in blue for spin up and light red for spin down). If the tunneling between the wires conserves the spin, we get a simple construction for inte-

ger, Laughlin-like, and non-Abelian topological insulators [32]. We note that other processes, which may not conserve spin, are possible. This can give rise to additional topological states.

*Generalization:* The approach we present here can be extended to hierarchical Abelian states, as well as other non-Abelian states (such as a Moore-Read-like state). One can also study the effects of proximity to a superconductor, which is expected to yield other non-Abelian states. A detailed further study of these constructions will be performed in the future.

*Experimental realizations:* The above theoretical construction may also be applicable in experiments with superlattices that realize the particle-hole structure we suggest. The alternating magnetic field can be generated using a snake-like wire [33]. For more details see the supplemental material [29]. We note that stripes with an alternating magnetic field can be realized in cold atom systems [34].

By coupling many (or maybe only a few) wires together we get an effective 2D system. Our construction lacks the disadvantages of fractional 1D states [21, 22], which are not topologically protected [35, 36], and the need to invoke proximity to a superconductor and a strong magnetic field simultaneously in 2D [23–25]. As long as the width of the edge modes is smaller than the sample width, it behaves practically as a topologically protected 2D system.

*Acknowledgments* We would like to thank Arbel Haim, Erez Berg, Eran Sela, Ady Stern, Netanel Lindner, Anna Kesselman for useful discussions. The work was supported by WIS-TAMU, ISF, Minerva and ERC (FP7/2007-2013) 340210 grants.

- 
- [1] K. Klitzing, G. Dorda, and M. Pepper, *Physical Review Letters* **45**, 494 (1980).
  - [2] D. Thouless, M. Kohmoto, M. Nightingale, and M. den Nijs, *Physical Review Letters* **49**, 405 (1982).
  - [3] F. D. M. Haldane, *Physical Review Letters* **61**, 2015 (1988).
  - [4] B. Halperin, *Physical Review B* **25**, 2185 (1982).
  - [5] Note that since the transition between different regions is affected by the details of the model, we expect the Bohr-Sommerfeld quantization condition to provide bands which are not flat in general.
  - [6] V. Yakovenko, *Physical Review B* **43**, 11353 (1991).
  - [7] S. Sondhi and K. Yang, *Physical Review B* **63**, 054430 (2001).
  - [8] C. Kane, R. Mukhopadhyay, and T. Lubensky, *Physical Review Letters* **88**, 036401 (2002).
  - [9] S. A. Parameswaran, R. Roy, and S. L. Sondhi, *Comptes Rendus Physique* **14**, 816 (2013).
  - [10] E. Tang, J.-W. Mei, and X.-G. Wen, *Physical Review Letters* **106**, 236802 (2011).
  - [11] K. Sun, Z. Gu, H. Katsura, and S. Das Sarma, *Physical Review Letters* **106**, 236803 (2011).



- [12] T. Neupert, L. Santos, C. Chamon, and C. Mudry, *Physical Review Letters* **106**, 236804 (2011).
- [13] D. N. Sheng, Z.-C. Gu, K. Sun, and L. Sheng, *Nature communications* **2**, 389 (2011).
- [14] Y.-F. Wang, H. Yao, Z.-C. Gu, C.-D. Gong, and D. N. Sheng, *Physical Review Letters* **108**, 126805 (2012).
- [15] N. Regnault and B. A. Bernevig, *Physical Review X* **1**, 021014 (2011).
- [16] X.-L. Qi, *Physical Review Letters* **107**, 126803 (2011).
- [17] S. A. Parameswaran, R. Roy, and S. L. Sondhi, *Physical Review B* **85**, 241308 (2012).
- [18] J. C. Y. Teo and C. L. Kane, (2011), [arXiv:1111.2617](#).
- [19] M. H. Freedman, M. J. Larsen, and Z. Wang, *Communications in Mathematical Physics* **228**, 177 (2002).
- [20] M. H. Freedman, M. Larsen, and Z. Wang, *Communications in Mathematical Physics* **227**, 605 (2002).
- [21] Y. Oreg, E. Sela, and A. Stern, (2013), [arXiv:1301.7335](#).
- [22] J. Klinovaja and D. Loss, (2013), [arXiv:1311.3259](#).
- [23] N. H. Lindner, E. Berg, G. Refael, and A. Stern, *Physical Review X* **2**, 041002 (2012).
- [24] A. Vaezi, (2013), [arXiv:1307.8069](#).
- [25] R. S. K. Mong, D. J. Clarke, J. Alicea, N. H. Lindner, P. Fendley, C. Nayak, Y. Oreg, A. Stern, E. Berg, K. Shtengel, and M. P. A. Fisher, (2013), [arXiv:1307.4403](#).
- [26] J. Klinovaja and D. Loss, (2013), [arXiv:1305.1569](#).
- [27] J. Klinovaja and D. Loss, *Physical Review Letters* **111**, 196401 (2013).
- [28] T. Neupert, C. Chamon, C. Mudry, and R. Thomale, (2014), [arXiv:1403.0953](#).
- [29] See supplemental material.
- [30] J. K. Jain, *Composite Fermions* (Cambridge University Press, 2007) p. 560.
- [31] P. Lecheminant, A. O. Gogolin, and A. A. Nersisyan, *Nuclear Physics B* **639**, 502 (2002).
- [32] M. Levin and A. Stern, *Physical Review Letters* **103**, 196803 (2009).
- [33] G. Zeltzer (private communication).
- [34] M. Aidelsburger, M. Atala, S. Nascimbène, S. Trotzky, Y.-A. Chen, and I. Bloch, *Physical Review Letters* **107**, 255301 (2011).
- [35] L. Fidkowski and A. Kitaev, *Physical Review B* **83**, 075103 (2011).
- [36] A. M. Turner, F. Pollmann, and E. Berg, *Physical Review B* **83**, 075102 (2011).

## SUPPLEMENTAL MATERIAL

The supplemental material contains more details about the tight binding model introduced in the main text. A detailed derivation of the  $m - \varphi$  phase diagram (Fig. 1d) is presented. In addition, we show explicitly how our construction of a non-Abelian state is mapped to the self-dual Sine-Gordon model, and provide technical details about the experimental realization suggested at the concluding part of the main text.

### TIGHT BINDING MODEL

The unit cell of the model is larger than the basic unit cell of the underlying square lattice: each unit cell contains 4 points, corresponding to the 4 different wires in Fig. 1b of the main text. Each point is characterized by  $(x, y)$ , the location of the unit cell (measured in units of the lattice spacing  $a$ ), and an index  $n = 1, 2, 3, 4$  which labels the sites inside the unit cell.

We define the annihilation operators,  $c_n(x, y)$ , in terms of which the tight binding Hamiltonian described in the main text is a sum of the following terms:

$$H_m = m \sum_{x,y} \left[ \sum_{n=1}^2 c_n^\dagger(x, y) c_n(x, y) - \sum_{n=3}^4 c_n^\dagger(x, y) c_n(x, y) \right], \quad (4)$$

$$H_y = -t \sum_{x,y} \left[ c_2^\dagger(x, y) c_1(x, y) + c_4^\dagger(x, y) c_3(x, y) + h.c. \right], \quad (5)$$

$$H'_y = -t' \sum_{x,y} \left[ c_3^\dagger(x, y) c_2(x, y) + c_1^\dagger(x, y+4) c_4(x, y) + h.c. \right], \quad (6)$$

$$H_x = -t_x \sum_{x,y} \left[ c_n^\dagger(x+1, y) c_n(x, y) e^{i\phi_n} - c_n^\dagger(x+1, y) c_n(x, y) e^{i\phi_a} + h.c. \right], \quad (7)$$

with  $\phi_1 = \phi_4 = -k_\varphi a = \varphi/2$  and  $\phi_2 = \phi_3 = k_\varphi a = -\varphi/2$ .

It is convenient to move to Fourier space, where the Hamiltonian takes the form  $H = \sum_{\mathbf{k} \in BZ1} \psi^\dagger(\mathbf{k}) h(\mathbf{k}) \psi(\mathbf{k})$ , with  $\psi = (c_1, c_2, c_3, c_4)^T$ , and

$$h(\mathbf{k}) = \begin{pmatrix} m - 2t_x \cos[(k_x - k_\varphi) a] & -t & 0 & -t' e^{4ik_y a} \\ -t & m - 2t_x \cos[(k_x + k_\varphi) a] & -t' & 0 \\ 0 & -t' & -m + 2t_x \cos[(k_x + k_\varphi) a] & -t \\ -t' e^{-4ik_y a} & 0 & -t & -m + 2t_x \cos[(k_x - k_\varphi) a] \end{pmatrix}. \quad (8)$$

We define a new gauge:

$$\begin{aligned} c_1(\mathbf{k}) &\rightarrow c_1(\mathbf{k}) e^{-ik_y a}, c_2(\mathbf{k}) \rightarrow c_2(\mathbf{k}) e^{-ik_y a}, \\ c_3(\mathbf{k}) &\rightarrow c_3(\mathbf{k}) e^{ik_y a}, c_4(\mathbf{k}) \rightarrow c_4(\mathbf{k}) e^{ik_y a}, \end{aligned} \quad (9)$$

in terms of which the Hamiltonian takes the simple form

$$\begin{aligned} h(\mathbf{k}) &= [m - 2t_x \cos(k_x a) \cos(k_\varphi a)] \sigma_z - 2t_x \tau_z \sin(k_x a) \sin(k_\varphi a) \\ &\quad - t \tau_x - t' \sigma_x [\cos(2k_y a) \tau_x - \sin(2k_y a) \tau_y], \end{aligned} \quad (10)$$

where  $\tau_i$  ( $i = x, y, z$ ) in Eq. (10) are Pauli matrices which operate within the  $2 \times 2$  blocks separately, while  $\sigma_i$  are Pauli matrices which operate on the outer  $2 \times 2$  matrix of blocks.

### Symmetries

It is easy to check that the Hamiltonian in Eq. (10) has a particle-hole symmetry,

$$\Lambda h(\mathbf{k}) \Lambda = -h^*(-\mathbf{k}), \quad (11)$$

where  $\Lambda = \sigma_x \tau_z$ . The particle-hole symmetry implies that the bands are symmetric around  $E = 0$ . Therefore, any crossing of the upper and lower bands must be at  $E = 0$ . Additionally, we have an inversion symmetry,

$$P h(\mathbf{k}) P = h(-\mathbf{k}), \quad (12)$$

where  $P = \tau_x$ . The crossings therefore must either be at the high symmetry points, satisfying  $-\mathbf{k} = \mathbf{k} + \mathbf{G}$ , or come in pairs.

### Crossing points

For convenience, we write the Bloch Hamiltonian, Eq. (10), in the form

$$h = A\sigma_z + B\tau_z + C\tau_x + D\sigma_x\tau_x + E\sigma_x\tau_y. \quad (13)$$

In terms of these, the spectrum is

$$E = \pm \sqrt{(A^2 + B^2 + C^2 + D^2 + E^2) \pm 2\sqrt{A^2 B^2 + A^2 C^2 + C^2 D^2}}. \quad (14)$$

Using this explicit form, it is now easy to find that the upper and lower bands cross each other at the high symmetry points when

$$m = \pm 2t_x \cos(k_\varphi a) \pm \sqrt{t^2 - t'^2}. \quad (15)$$

These crossing points signal a topological phase transition between a topologically trivial phase and a phase with a non-zero chern number.

There are additional crossings at the points  $k_\varphi a = 0, \pi$ , whose locations depend on  $m$ . Since these crossings are not at the high symmetry points, they must come in pairs.

If we add a small non-zero chemical potential  $\mu$ , the bands cross the chemical potential when

$$m = \pm 2t_x \cos(k_\varphi a) \pm \sqrt{(t \pm \mu)^2 - t'^2}. \quad (16)$$

The topologically trivial and non-trivial insulating phases are now separated by metallic phases. The transitions between the metallic and insulating phases are described by Eq. (16).

In the same way, metallic regions appear near  $k_\varphi a = 0, \pi$ .

### MAPPING TO THE SELF-DUAL SINE-GORDON MODEL

In terms of the bosonized  $\eta$  fields, the scattering terms presented in the main text are:

$$v [\cos(\eta_2^L - \eta_1^R) + \cos(\eta_3^R - \eta_4^L) + \{2 \leftrightarrow 4\}]. \quad (17)$$

Defining  $(\phi_c, \theta_c, \phi_s, \theta_s)^T = U (\eta_4^L, \eta_1^R, \eta_2^L, \eta_3^R)^T$ , with  $U = \frac{1}{\sqrt{24\pi}} (\sigma_x + \sigma_z) \otimes (\sigma_x + \sigma_z)$  (where  $\sigma_i$  are the pauli matrices), we can write the Hamiltonian in the convenient form

$$\int \left[ \frac{1}{2} \sum_{a=c,s} \left( (\partial_x \phi_a)^2 + (\partial_x \theta_a)^2 \right) + 2 \cos(\sqrt{6\pi} \theta_c) \times \right. \\ \left. v [\cos(\sqrt{6\pi} \theta_s) + \cos(\sqrt{6\pi} \phi_s)] \right] dx dt. \quad (18)$$

The term  $\cos(\sqrt{6\pi} \theta_c)$  is relevant, and  $\theta_c$  is therefore frozen at a minimum. This allows us to treat  $\cos(\sqrt{6\pi} \theta_c)$  as a constant.

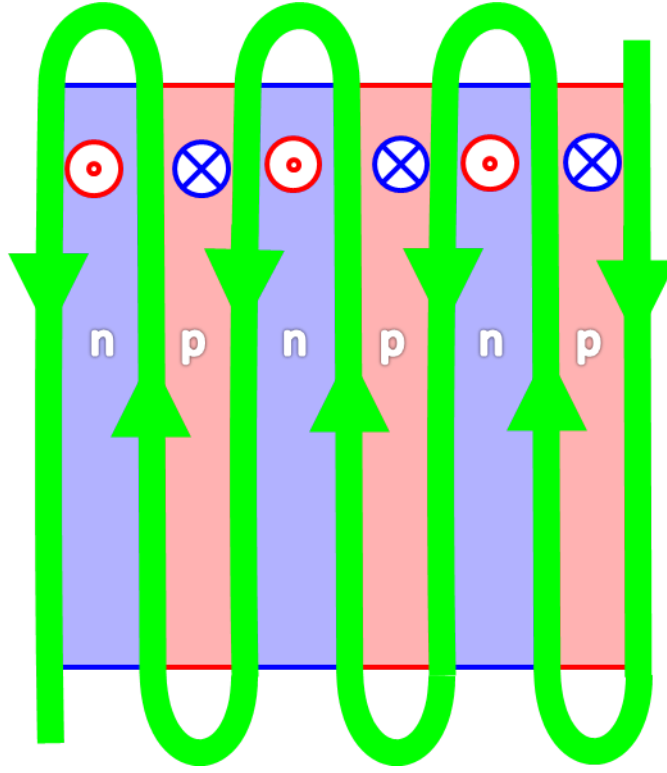


FIG. 3. A possible experimental realization of our construction. Green lines represent current carrying wires, which produce the alternating magnetic field needed for our construction. This way, the magnetic field is positive (i.e. out of the page, denoted by  $\odot$ ) in  $n$ -regions that contain electrons, and negative ( $\otimes$ ) in  $p$ -regions that contain holes.

### EXPERIMENTAL REALIZATION

Our Q1D construction requires an alternating magnetic field. Experimentally, this can be realized using a snake-like wire, similar the one shown in Fig. 3.

In this configuration, we get that the desired current needed to create the states we constructed is of order

$$I \sim \frac{n\pi\hbar c^2}{2e} \approx 100mA \frac{n}{(100nm)^{-1}},$$

where  $n$  is the one-dimensional density of the conducting band. Assuming  $n^{-1} \sim 100nm$ , we get that currents of order  $\sim 100mA$  should suffice.